

Electrical Properties of Meso-Porous Silicon: from a Surface Effect to Coulomb Blockade and More

L. Boarino, S. Borini and G. Amato

Electromagnetic Division, Istituto Nazionale Ricerca Metrologica
Strada delle Cacce, 91 – 10135 Turin, Italy

Since the Volker Lehmann's paper "Resistivity of Porous Silicon: a surface effect" published in 1995, a great deal of effort has been produced in understanding the basic mechanisms ruling the electron transport in Si mesostructures and how these phenomena are affected by external environment. After more than 10 years, new experimental evidences and physical insights have been obtained, like gas sensitivity, chemisorptions phenomena, Coulomb blockade and glassy dynamics at room temperature, but reading that former paper, the feeling of an extraordinary comprehension and intuition of the physical phenomena occurring in this fascinating material is continuously accompanying the reader.

A review of these major results in studying electronic transport in mesoporous silicon will be reported, starting from the still valid intuitions of Volker Lehmann in his paper.

Introduction

In the first half of the '90s, the most studied porous silicon morphology was from high resistivity p-type wafers, because of the high luminescence efficiency. The former studies on electrical and transport properties of nano¹ and mesoporous² silicon (mesoPS), revealed a resistivity of the porous layer of few orders of magnitude higher than the original substrate. The models proposed to explain these first results were based on quantum confinement³ and on the dielectric constant variation⁴, but they were strictly applicable to luminescent, confined structures, rather than to mesoporous silicon from highly doped silicon. The Lehmann's paper on electrical properties of porous silicon from p+ doped wafers, addressed few unanswered crucial questions regarding resistivity, impurity role, carrier freeze out and surface conditioning, proposing a microscopic model of transport in mesoPS, in which also in a broader size distribution, typically a log-normal between 4 and 12 nm⁵, where quantum confinement is not observed, the effect of trapped charges at surface and the interaction of single charges result in a blocking of conduction mechanisms.

High resistivity of mesoPS

One of the most inspiring idea of the Lehmann's paper is the analogy of mesoporous silicon structures to submicron channels of CMOS devices, whose figures of telegraph noise are due to single charge trapping at the oxide-semiconductor interface. Telegraph noise is a screening effect manifesting in submicron CMOS channels, ascribable to the capture and emission from a trap at the silicon-oxide interface in gate region, so blocking part of the channel to electrical conduction. A parallel with silicon nanowires in a mesoporous structure was proposed, in which charged surface traps result in carrier constrictions or blockade at room temperature.

Another evidence in support of this hypothesis was the almost complete transparency to IR light of the material after etching, while in the original form the highly doped substrates are opaque, due to the absorption from free carriers. So, an interesting question was, like Polissky et al.⁶ titled in one of their papers: “Boron in mesoporous Si - Where have all the carriers gone?”

In this work the authors proposed, on the basis of detailed ERDA and SIMS studies, that despite the electrical and optical evidence of complete absence of free carriers, the Boron is still present after etching, the electrochemical process does not selectively remove these impurities, (vice versa at high porosities the boron content increases respect to silicon atoms) so the most plausible explanation resides in the presence of saturated dangling bonds. These centers, also called Pb centers⁷ have been observed by Electron Spin Resonance (ESR) by different groups^{8,9} and could be the responsible of the high resistivity of mesoporous silicon. These authors also proposed a mechanism affecting the PS formation and morphology, in which boron impurities remain passivated in near-surface sites, while the etching proceeds removing silicon atoms not in vicinity of impurities. This picture could also justify the different size distribution of crystallites in mesoPS.

Surface effects

Lehmann also focused his attention of the interaction between mesoPS and environment, in particular in polar gases and liquids, like water and ethanol^{4,10}, to validate his model, in fact the condensation of these two vapors or the direct immersion in these two liquids give origin to an increase of conductivity, explained by Tsu and Babic¹¹ in terms of an increase of effective dielectric constant. The interaction with liquid ethanol was then addressed by a detailed study of Timoshenko¹².

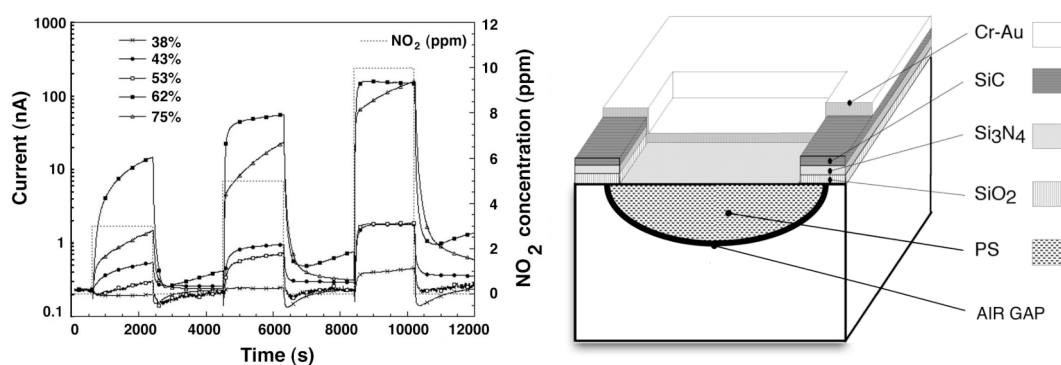


Figure 1. Left: electrical response to controlled concentrations of NO₂ (3, 5, 10 ppm) of one of the former group of mesoPS sensors as a function of time and plotted for increasing porosities. Right: the fabrication scheme of a front-side micromachined mesoPS sensor.

In the same period, the first report of a sensitivity of PS to NO₂ appeared in literature, by Harper and M.J. Sailor¹³. They were using n type nanoporous silicon obtained by front illumination, but the effect of exposure to nitrogen dioxide was not reversible.

MesoPS and nitrogen dioxide

In 1999, a strong interaction between mesoporous p+ silicon was announced in

Strasbourg, EMRS by our group¹⁴. Volker Lehmann was chairman of that session, and he was sincerely interested in the electrical and infrared striking response of this material to nitrogen dioxide.

In fig.1 (left) the current response of different porosity samples of mesoPS, contacted by chromium gold pads in planar configuration, is shown, plotted versus exposure time. The right axis reports the NO₂ concentration, and the thin continuous line refers to the different gas dosage in the chamber. The samples were constantly biased to 5 V.

The response appears to be related to specific surface through porosity, with a maximum around 62%, as reported by previous studies¹⁵. But our feeling already in that period was that structures dimension are more meaningful than porosity.. The response to gas was anyway impressive, more than one order of magnitude in current variation for 1 ppm, a sensitivity never reported with any other gas or liquids. Another striking feature of the data was the response time, composed of a sharp and quick response on the rising front, and a slower component, never reaching stability or saturation in the flat part of the step. Also during gas evacuation, a peculiar and undesired drift in response was observed on the visualized time scale.

While a technological CMOS compatible process was easily proposed in 2001¹⁶ for the front-side fabrication of a porous silicon NO₂ sensor, with a new record in sensitivity obtained by means of a self-suspended membrane of PS (Fig. 1, right), the origin of such an high sensitivity, was still unclear. The active element, mesoPS, was

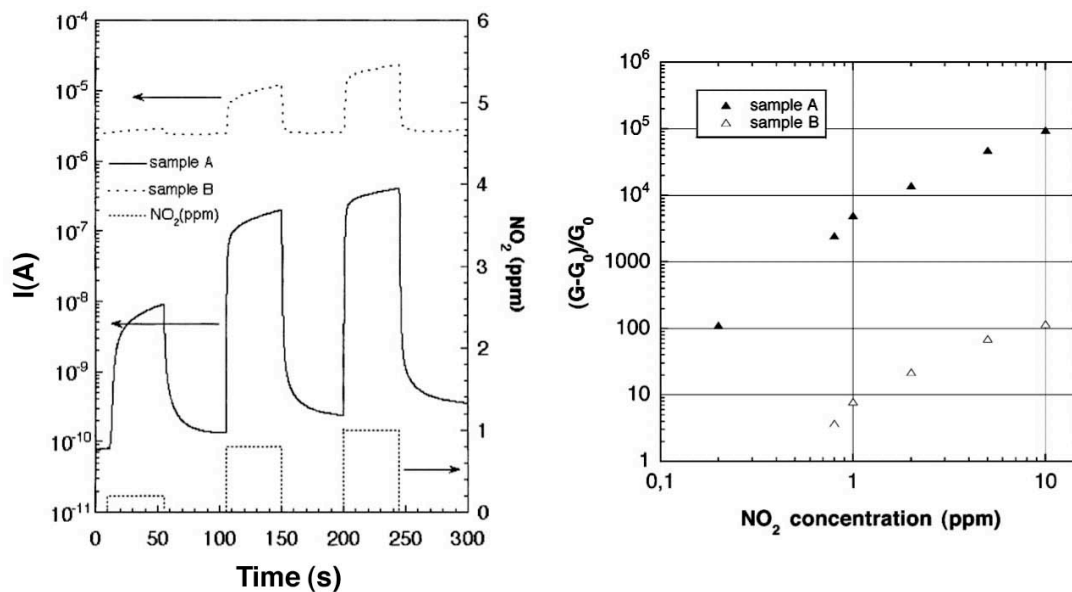


Figure 2. Left: electrical response vs time of a front-side micromachined NO₂ sensor for NO₂ dosage of 200, 800 ppb and 1 ppm. Right: comparison between the electrical response of a suspended membrane PS sensor and a PS layer still attached to crystalline substrate is shown, for NO₂ concentrations ranging from 200 ppb (alarm level for EU legislation) to 10 ppm.

obtained opening a window in the passivation layers, then performing electrochemical etching of mesoPS formation, and stopping the etching with few seconds of high current density, working in electropolishing regime. A mesoporous membrane is so obtained, sustained by the passivation layers, also thanks to the under-etching.

In Fig.2, the electrical response of a front-side micromachined NO₂ sensor is presented. The comparison between the electrical response of a suspended membrane PS sensor and a PS layer still attached to crystalline substrate is shown, for different NO₂ concentrations ranging from 200 ppb (alarm level for EU legislation) to 10 ppm. More than two orders of magnitude in relative conductance (G-G₀)/G₀ in presence of

1 ppm of NO_2 are obtained respect to the normal configuration. These first indications on the response of free-standing and electrically insulated structures were important to improve the device performances, but the origin of the reactivity was still unclear.

FTIR studies

In conjunction with the investigation on the electrical properties, in-situ IR spectroscopy was carried on, revealing another impressive feature of the interaction phenomenon. The FTIR spectra of freshly prepared mesoPS have been widely reported in literature¹⁷, and the major characteristics were well known, but a study on the spectral evolution in controlled environment was still lacking. The first FTIR measurements of fresh meso PS in presence of NO_2 were impressive, since a featureless absorption, characteristic of a loss of transparency of the sample, occurred at NO_2 exposure, with an almost fully reversible effect during gas evacuation. The typical spectral features related to Si-Hx stretching and SiO-H modes, were not apparently affected by this dramatic optical response. The behavior is visible in Fig. 3, the solid line 1 is the fresh sample in vacuum, the dashed line 2 is in presence of 1Torr of pure NO_2 , and the dotted line 3 has been acquired after gas evacuation. It is interesting, and not yet understood, the complete return to initial conditions (curve 1) only after exposure to air.

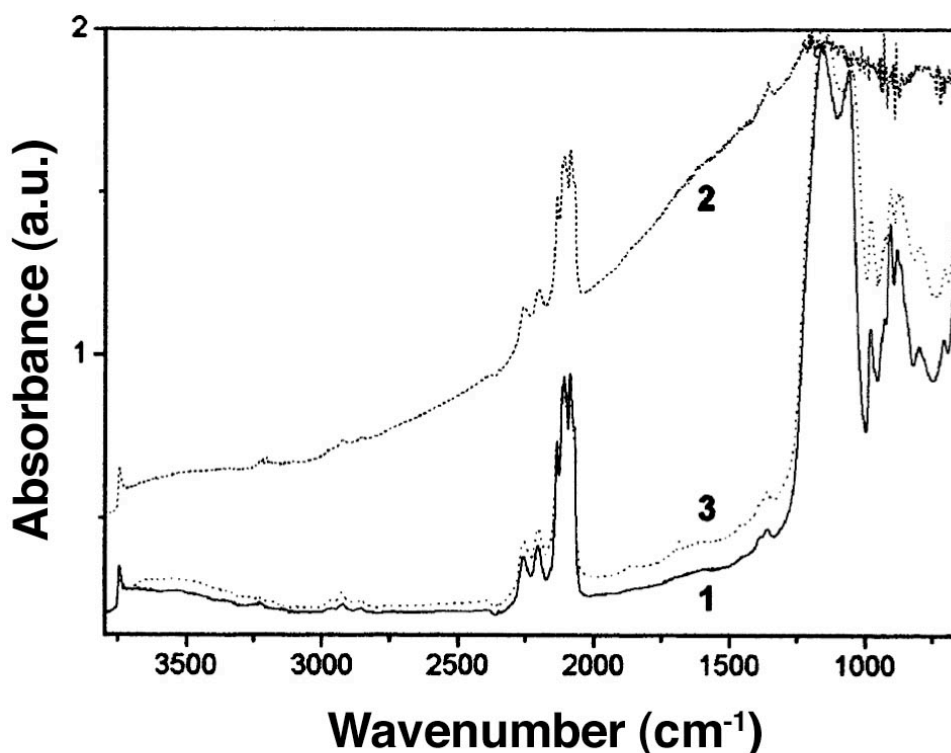


Figure 3. FTIR spectra of mesoPS exposed to nitrogen dioxide. The solid line 1 is the fresh sample in vacuum, the dashed line 2 is in presence of 1Torr of pure NO_2 , and the dotted line 3 has been acquired after gas evacuation.

This loss of transparency was immediately attributed to the optical absorption of free carriers, in some way reactivated by interaction with nitrogen dioxide, whose electron affinity is rather high, 2.2 eV respect to other gases and molecules.

The successive years were so devoted to a fundamental study of mesoporous silicon in interaction with gas, by means of IR spectroscopy¹⁸¹⁹, ESR²⁰, NMR and ab-initio calculations,²¹²² in order to understand the basic mechanisms at the origin of

such an impressive optical and electrical response to nitrogen dioxide and also ammonia, another probe gas capable to easily donating an electron, and the role of impurities and morphology in these phenomena.

Other techniques and results

Since our former paper of 1999, other groups contributed to study the NO₂ interaction with detailed papers on IR spectroscopy and Drude effect due to free carriers restored by nitrogen dioxide²³ and obtaining new records of sensitivity²⁴ (15 ppb in dry air).

The main results of this period of fundamental investigations were the following²¹:

- meso Porous Silicon is by the electrical point of view, a near-insulator and becomes either a p- or an n-type semiconductor upon gas adsorption (NO₂ and NH₃)
- the interaction between these two probe gas is stronger than those typical of polar gases and liquids, is well represented by an adsorption isothermal characteristic of a chemisorption mechanism
- The effect of free carriers deactivation/reactivation is reversible at low concentration of these two gases, and it's not due to a changing in coordination of the boron impurities at the mesostructure surface.

Electrical anisotropy and Coulomb Blockade

Since 2005, our work continued focusing the investigation on electron transport phenomena in mesoPS in interaction with probe gases. Thanks to new experimental set-ups, new aspects of the complex phenomena were understood and demonstrated.

The experimental setup shown in the inset of Figure 4, allowed the demonstration of electrical anisotropy in p+ mesoPS morphology²⁵, only demonstrated, in the same period, for (110) wafers by Timoshenko et al.²⁶, and always given as an assumption, but never measured and separated in two different contributions, longitudinal (I_L) and transversal (I_T) to the (100) direction.

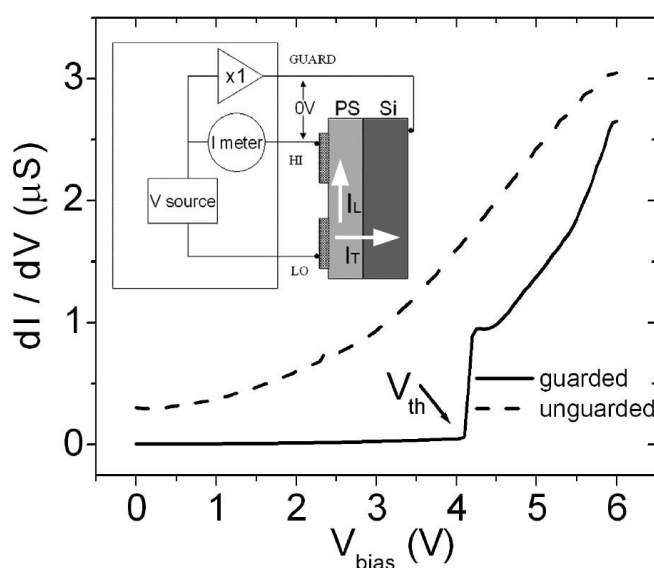


Figure 4. Differential conductance of a mesoPS sample (60% porosity). A gap characterized by a threshold voltage is clearly visible. When the guard is removed, the gap disappears. This is related to the structural anisotropy of mesoPS. The inset shows the measurement configuration.

As depicted in the scheme of Fig. 4, when a bias voltage is applied between the coplanar contacts, the measured current I is given by the sum of the longitudinal current I_L crossing mesoPS from one pad to the other, i.e., parallel to the (100) plane and the leakage current I_T , unless the backside contact is used as guard electrode. In the latter case, the same potential is kept on the backside contact and on one planar contact, so that no current flow occurs between them.

Measuring the samples in both the configurations is possible to separate the different conductivity contributions in the case of a strongly anisotropic material like p^+ mesoporous silicon. In the case of isotropic nanoporous silicon the two components would result indistinguishable.

The room temperature conductivity in the transverse direction appears to be already percolated, while the longitudinal direction appears to be strongly inhibited. This difference disappears increasing the temperature from 20 to 100 ° C, with a longitudinal conductivity rise of about six orders of magnitude. The strong electrical anisotropy measured in this material gives a further confirmation of the former results of increased sensitivity in the suspended PS membranes of 2001¹⁵.

Furthermore, all the mesoPS samples under investigation showed, in guard electrode configuration, the presence of a sharp threshold voltage V_{th} in the current–voltage (I – V) characteristics at RT. The typical gap in the conductance observed for a sample of 60 % porosity is shown in Figure 4. As the guard contact is removed, the threshold disappears, since the conductive pathways are restored again along the transversal direction, already percolated, and the bottlenecks constituted by small nanoconstrictions are rare and easily bypassed.

Investigating the shape and dependence of the threshold voltage with temperature variation from room temperature to 200 K, it's been possible to understand the origin of the conductance gap, identifying an increasing of the threshold values with decreasing temperature, and a power-law behavior for $V > V_{th}$ common to other metallic or semiconducting nanoparticle systems like Co nanocrystal superlattices²⁷, Au nanocrystal arrays^{28,29}, GaAs quantum dots³⁰, PbSe quantum dots³¹, C nanoparticle chains³², and polymer nanofibers³³. [20] Moreover, such a behavior was theoretically predicted by Middleton and Wingreen (MW)³⁴[21] for the collective transport in arrays of small metallic dots.

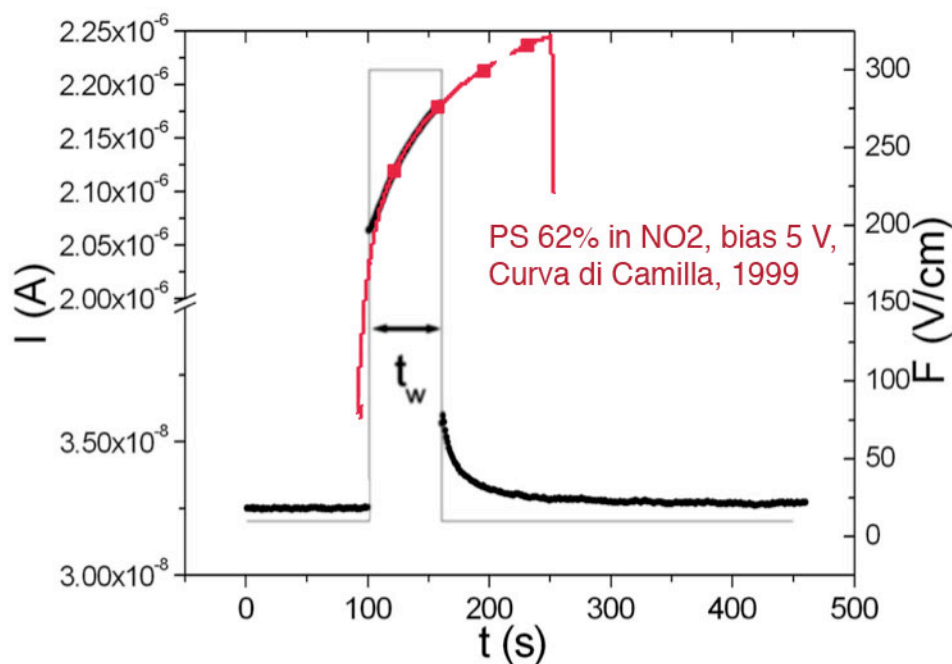
The smaller interconnecting nanostructures parallel to the plane 100 have a very low capacitance, and if charged, the repulsive energy barrier exceed the thermal energy at a given temperature, event RT. The charge flow in this path is than blocked by Coulomb repulsion. Temperature and NO_2 have the capability to pin this CB gap.

This strong dependence of electrical transport in PS from Coulomb blockade was taken in account from V. Lehmann in his model, then predicted by Hamilton³⁵ and coworkers in 2000, but never demonstrated before.

Conclusions

The most recent chapter of the story is the experimental observations of intriguing time-dependent charge transport phenomena, such as slow conductivity relaxation, nonergodicity, and simple aging at room temperature³⁶. These phenomena have a deep impact on transport in mesoPS, affect the electrical response of the material to gases, with a typical and well defined fingerprint.

Questa figura non la metto, ma vi da' un'idea di cosa intendo nelle righe precedenti....



The Lehmann's deep intuitions, after 13 years from his paper on these topics, and 2 years from his early departure, still hold true, and new areas of investigation are emerging thanks to the deeper comprehension gained also thanks to his first indications.

Acknowledgments

Place acknowledgments at the end of the text, before the references.

References

1. T. Unagami, *J. Electrochem. Soc.* **127**, 476 (1980).
2. M. I. J. Beale, J. D. Benjamin, M. J. Uren, N. G. Chew and A. G. Cullis, *J. Cryst. Growth*, **73**, 622 (1985).
3. A. J. Read, R. J. Needs, K. J. Nash, L. T. Canham, P. D. J. Calcott and A. Qteish, *Phys. Rev. Lett.*, **69**, 1232 (1992).
4. R. Tsu and D. Babic, *Appl. Phys. Lett.*, **64** 1806 (1994).
5. L.T. Canham, *Properties of Porous Silicon*, p. 106., edited by L. T. Canham, EMIS Data review series, INSPEC, (1997)
6. G. Polisski, D. Kovalev, G. Dollinger, T. Sulima, F. Koch, *Physica B*, **273** 951 (1999)
7. E.H. Poindexter, P.J. Caplan, B.E. Deal, R.R. Razouk, *J. Appl. Phys.* **1981**, 52, 879.
8. H.J. von Bardeleben, D. Stievenard, A. Grosman, C. Ortega, J. Siejka *Phys. Rev. B* **1993**, 47, 10899.
9. F. C. Rong, J. F. Harvey, E.H. Poindexter, G.J. Gerardi, *Appl. Phys. Lett.* **1993**, 63, 920.

-
10. M. Ben-Chorin, A. Kux and I. Schechter, *Appl. Phys. Lett.*, **64** 481 (1994).
 11. R. Tsu, D. Babic, *Appl. Phys. Lett.*, **64** 1806 (1994)
 12. V. Yu. Timoshenko, T. Dittrich, V. Lysenko, M. G. Lisachenko, and F. Koch, *Phys. Rev. B*, **64**, 085314 (2001)
 13. J. Harper and M. Sailor, *Anal. Chem.*, **68**, 3713, (1996)
 14. L. Boarino, C. Baratto, F. Geobaldo, G. Amato, E. Comini, A. M. Rossi, G. Faglia, G. Lérondel, G. Sberveglieri, *Materials Science and Engineering B*, **69-70**, 210 (2000)
 15. Lavoro superficie specifica-porosità, Halimaoui Les Houches o INSPEC
A. Halimaoui, in *Porous silicon: material processing, properties and applications*, Les Houches, J.C. Vial, J. Derrien Eds., Les editions de physique Springer, pp. 33 (1994)
 16. C. Baratto, G. Faglia, G. Sberveglieri, L. Boarino, A. M. Rossi, and G. Amato, *Thin Solid Films*, **391-392**, 261 (2001).
 17. Y. Ogata, H. Niki, T. Sakka, M. Iwasaki, *J. Electrochem. Soc.*, **142**, 1595 (1995)
 18. P. Rivolo, F. Geobaldo, M. Rocchia, et al., *Physica Status Solidi A*, **197**, 217 (2003).
 19. F. Geobaldo, P. Rivolo, M. Rocchia, et al., *Physica Status Solidi A*, **197**, 458 (2003),
 20. M. Chiesa, G. Amato, L. Boarino, E. Garrone, F. Geobaldo, and E. Giamello, *Angewandte Chemie Int. Ed.*, **42**, 5031 (2003)
 21. S. Borini, P. Ugliengo, *Physica Status Solidi A-Applied Research*, **197** 436 (2003)
 22. E. Garrone, F. Geobaldo, P. Rivolo, G. Amato, L. Boarino, M. Chiesa, E. Giamello, R. Gobetto, P. Ugliengo, A. Viale, *Advanced Materials*, **17**, 528 (2005)
 23. V.Y. Timoshenko, T. Dittrich, V. Lysenko, et al., *Physical Review B*, **64**, 8 (2001).
 24. L. Pancheri, C. J. Oton, Z. Gaburro Z, et al., *Sensors and Actuators B-Chemical*, **89**, 3, 237 (2003)
 25. S. Borini, L. Boarino, and G. Amato, *Applied Physics Letters*, **89**, 132111 (2006)
 26. P.A. Forsh, M.N. Martyshev, V. Y. Timoshenko, et al., *Semiconductors*, **40**, 471, (2006)
 27. C. T. Black, C. B. Murray, R. L. Sandstrom, S. Sun, *Science*, **290**, 1131. (2000)
 28. H. Fan, K. Yang, D. M. Boye, T. Sigmon, K. J. Malloy, H. Xu, G. P. Lopez, C. J. Brinker, *Science*, **304**, 567. (2004)
 29. R. Parthasarathy, X.-M. Lin, K. Elteto, T. F. Rosenbaum, H. M. Jaeger, *Phys. Rev. Lett.*, **92**, 801, (2004)
 30. C. I. Duruoaz, R. M. Clarke, C. M. Marcus, J. S. Harris, *Phys. Rev. Lett.*, **74**, 3237 (1995)
 31. H. E. Romero, M. Drndic, *Phys. Rev. Lett.*, **95**, 801, (2005)
 32. A. Bezryadin, R. M. Westervelt, M. Tinkham, *Appl. Phys. Lett.*, **74**, 2699 (1999)
 33. A. N. Aleshin, H. J. Lee, S. H. Jhang, H. S. Kim, K. Akagi, Y. W. Park, *Phys. Rev. B*, **72**, 202 (2005)
 34. A. A. Middleton, N. S. Wingreen, *Phys. Rev. Lett.*, **71**, 3198 (1993)
 35. B. Hamilton, J. Jacobs, D.A. Hill, et al., *Nature*, **393**, 443 (1998)
 36. S. Borini, L. Boarino, G. Amato, *Phys. Rev. B*, **75**, 165205 (2007)